Role of Atlantic SST in the Recent ENSO Predictability Change in NMME Model Hindcasts

Prasanth A Pillai (prasanthap2@yahoo.co.in)
Indian Institute of tropical meteorology https://orcid.org/0000-0002-8159-6066
Ashish R Dhakate
Indian Institute of Tropical Meteorology

Research Article

Keywords: ENSO predictability, North Atlantic SST, Atlantic Nino, Potential skill, Actual skill

Posted Date: October 20th, 2021

DOI: https://doi.org/10.21203/rs.3.rs-987430/v1

Abstract

The present study analyses the possible change in the seasonal prediction skill of El Nino Southern Oscillation (ENSO) in association with the reported climate modification in the tropical Pacific during the early 21st century. The hindcasts of nine models that participated in the National Multimodel Ensemble Project (NMME) are used for the analysis. Both the boreal summer (JJAS) and winter (DJF) seasons ENSO indices from 4 months and 1-month lead for the period 1981-2018/19 are studied. The analysis shows that all the models have reduced interannual variability as observations for both seasons. There is not much skill (both actual and potential) difference for DJF season for all the models for both the lead times. Summer skill loss for Feb IC is more for models such as CanSIPv2, CCSM3 and NEMO, while it is minimum for CCSM4. There is an increase of skill for Feb IC hindcasts for three GFDL models for JJAS season. Most of the models failed to simulate the ENSO events during the second period. The summer season ENSO pattern in the recent period are influenced by spring time north Atlantic SST anomalies. The models with maximum decrease of skill after 2000 fail to simulate the tropical Atlantic SST anomalies during the initialization months and also the summer season SST anomalies induced by these SST anomalies. The models with better or close to observed patterns with Atlantic SST induced ENSO patterns are only able to maintain the same skill as previous decades.

Introduction

El Nino Southern Oscillation (ENSO) is the climate phenomenon impacting the climate around the world with impacts on health, agriculture, water resources and ecosystem (McPhaden et al. 2006). Fortunately, the occurrence of ENSO can usually be predicted 2-3 seasons ahead using modern operational seasonal prediction systems (e.g., Barnston et al. 2012), which help in preparing for the ENSO impacts. This achievement is made as a result of the improvement in observations made during the last 2 decades (Balmaseda et al 2007) and the better scientific understanding of ENSO mechanism and improved modelling systems developed by different forecasting centres around the world (Balmaseda et al 2013, Saha et al 2014, Zhao et al 2013, 2014). The accurate prediction of global climate also depends on the precise long-term predictability of ENSO. Recent studies (Barnston et al 2012, Kumar et al 2015) using different seasonal prediction models have shown that the long-lead predictability of ENSO has declined in the early twenty-first century compared to the last decades of the previous century. This is a typical issue, which may have an impact not only on the predictability of Pacific SST and climate but also on world climate as a whole.

Meanwhile observed climate of the tropical Pacific also has undergone modifications in the 21st century. Feng et al. (2010) and McPhaden et al. (2011) showed that there is a strong background state change during the first decade of the twenty-first century with stronger trade winds, shallower thermocline and cool SST in the eastern Pacific. These variations resulted in different flavours of ENSO in which the central Pacific ENSO (ENSO Modoki, Ashok et al. 2007) is more robust in the recent periods (McPhaden et al. 2011, Chung and Li 2013). Luo et al. (2012) also reported that in the recent periods, La Niña like background state prevails in the equatorial Pacific. Chung and Li (2013) showed that this La Niña like the interdecadal basic state is responsible for central Pacific El Niño in the recent period. They showed that due to the increase of background zonal SST gradient, the convection associated with the background zonal SST shifts more westward inducing central Pacific ENSO more than east Pacific ENSO. Hu et al (2013) reported a decrease in the interannual variability of tropical east Pacific SST along with a weaker and irregular ENSO (Wen et al 2014). This is associated with a drop in signal to noise ratio (Barnston et al 2012, Kumar et al 2015). There is also a change in Interdecadal Pacific Oscillation (IPO) from positive to negative phase (Chung and Li 2013, Xinag et al 2013) in the early 2000s. This change in the IPO phase coincides with the shift in ENSO skills also. Furthermore, the lead-lag relationship between ENSO and the recharge/discharge of heat across the equatorial Pacific, which is a significant reason for the long-lead predictability of ENSO (Jin et al 1997), was also weakened and is shorter in the current period (Mc Phaden et al 2012, Wen et al 2014). This decline also coincided with more frequent occurrences of Central Pacific El Niño (CP-ENSO) events, in which the SST warming is not only related to the thermocline feedback, but also some other extratropical processes.

Thus a natural climate change is observed in the tropical Pacific in the recent period, which can influence the properties of ENSO such as its interannual variability (IAV), frequency, amplitude etc which may be associated with basic state change in the tropics. Based on signal-to-noise principles, it is generally believed that ENSO predictability is related to the magnitude of ENSO variability (i.e., the larger its variability, the less likely that the ENSO signal). It is already proven that seasonal prediction models have a weaker ability to predict the central Pacific ENSO than the east Pacific ENSO (Hendon et al 2009, Pillai et al 2017). There is also evidence that the negative IPO phase is associated with epochs of lower predictability for ENSO (Kirtman and Schopf 1998, Choi et al 2011, Hu et al 2013). Thus it is evident that there will be a change in ENSO skill between the two decades centred around 2000. The present study looks at the difference in ENSO skill in the National Multi-Model Ensemble Project (NMME, Kirtman et al 2013) models to understand the change in the predictive skill of ENSO, which can have a major role in the prediction of global climate. Here we are looking at the skill of ENSO for both its developing and mature phase, ie for boreal summer (JJAS) and boreal winter (DJF).

Along with natural variability of ENSO, it is shown that the ENSO variability is controlled by SST anomalies of both Indian and Atlantic Oceans also (Kug and Kang 2006, Luo et al 2010, Izumo et al 2016, Rodriguez-Fonseca et al 2009, Ham et al 2013a, b., Wang et al 2009 etc). Luo et al 2010 and Izumo et al 2016 showed that Indian Ocean SST plays a role in determining the phase reversal of ENSO in the flowing year.

Meanwhile, other studies with Atlantic SST anomalies have shown that two types of Atlantic SST anomalies can influence ENSO evolution. The north Atlantic SST anomalies (SST anomalies averaged over the area 90^0W-20^0E, 0^0-15^0N of the tropical Atlantic) during the spring season is supposed to influence the evolution of ENSO in the tropical Pacific. Ham et al (2013b) have shown that the ENSO associated with these north Atlantic SST anomalies are mainly central Pacific ENSO events as there is a cancellation of wind anomalies occur over the east Pacific that induced by the north Atlantic SST and evolving ENSO. Meanwhile, the north Atlantic SST anomalies are influenced by the previous year ENSO conditions also. Studies such as Rodriguez-Fonseca et al (2009), Ham et al (2013a, b)., Wang et al (2009) have also shown that the equatorial Atlantic SST anomalies in the form of Atlantic Nino also influence the ENSO evolution. These SST anomalies contribute to canonical ENSO through the modification of Walker Circulation. Another important finding is that these relationships are not stationary and is found to be strong after the 1990s only. Thus, it may be interesting to look at the variation of influence of these SST anomalies on ENSO during the two periods along with the changes that occurred in the Pacific basin to understand the recent variations in ENSO predictability.

2. Data And Methodology

The present study mainly uses SST data from different models that participated in National Multi-Model Comparison Project (NMME, Kirtman et al 2013) for the period 1981-2019. The NMME is a multimodel forecasting system consisting of a series of coupled climate models from U.S. modelling centres, including NCEP, GFDL, NASA, NCAR, and the Canadian Meteorological Centre. In these models, whose hindcast is available up to at least 2018 is only taken in the present study as we have to consider two periods P1(1981-2000) and P2(2002-2018/19) as per the availability of the data. SST data for all these model hindcasts are available on the IRI data server: http://iridl.ldeo.columbia.edu/SOURCES/.Models/.NMME/., which hosts mainly SST and rainfall data sets only. All data has more than 10 ensembles and a lead time of more than 9months. Feb IC and May IC hindcasts are used for JJAS target season and Aug IC and Nov IC hindcasts are used for DJF season. Hadley Centre Global Sea Ice and Sea Surface Temperature (HadISST, Rayner et al 2003) for the same period is used to represent observed SST. Zonal and meridional wind at 850 hPa and velocity potential at 200 hPa level taken from the ERA reanalysis 5 (Hersbach et al 2020) are also used as observations.

The present study uses anomaly correlation of observed and model hindcast indices to identify the model's skill for two different periods 1981-2000 and 2002-2019. Nino3.4 (SST anomaly averaged over the region 5^0S-5^0N, 170^0W-120^0W) and Nino3 (SST anomaly averaged over 5^0S-5^0N, 120^0W-80^0W) to define ENSO. Central Pacific ENSO years are defined using El Nino Modoki index (EMI) using the criteria of Ashok et al (2007). The potential skill of these SST indices is calculated using each ensemble and followed the same method as Pillai et al (2018). Here relative entropy (RE) values based on information theory (Kleeman 2002) are used for calculating potential skill. RE values are calculated based on the assumption that forecast and observations are near Gaussian distributions and is governed by the equation

$$RE = \frac{1}{2}\left(\ln\left(\frac{\sigma^2_x}{\sigma^2_{xi}}\right) + \frac{\sigma^2_{xi}}{\sigma^2_x} + \frac{(\mu_{xi}-\mu_x)^2}{\sigma^2_x} - 1\right)$$

Here x denotes observations and xi denotes forecast/hindcast and σ^2 for variance and μ^2 for ensemble mean, which is only for model hindcasts. The first two terms on the right side of the RE equation will give contribution from model spread as these are dominated by model and observed variance and third term is governed by ensemble mean contributed by signal size to RE. Thus, RE will have value for every year and is a prognostic prediction parameter (Pillai et al 2018). Average of RE will give average predictability called as mutual information (MI) and potential skill is calculated from MI as

$$\text{Potential skill} = \sqrt{(1 - e^{(-2MI)})} \qquad -2$$

SST anomalies of north Atlantic (NA_SST, 90^0W-20^0E, 0^0-15^0N) and Atlantic Nino (ATL, 20^0W-0^0, 3^0S-3^0N) are used to find the influence of Atlantic Ocean on tropical SST. Regression analysis and composite analysis for both the periods are conducted to understand the role of different forcing. Long term seasonal trend is removed from all the data before performing the analysis.

3. Results

a) Mean Pacific SST state difference for individual models.

Table 1 below shows the SST bias and standard deviation for model hindcasts for both the seasons and lead hindcasts. In all the model hindcasts, the standard deviation (i.e., interannual variability) is decreased in the tropical Pacific (table 1) as similar to the observed decrease. Meanwhile, the mean SST difference between the two periods is not much significant for the model hindcasts, if the seasonal trend for the period is removed from the data (not shown). Similar to the observations, all the model hindcasts have decreased interannual variability of

ENSO for the second period irrespective of the initial condition and target season. Models such as CanCM4i, CanSIPSv2, CCSM3, CCSM4, GFDL_aero4, GMAO6 and NEMO has negative bias over the Nino3.4 region for all ICs but is reduced for the second period and is changed to positive bias for CCSM4. The positive bias of the second period is stronger for the DJF target season from both the Aug IC and Nov IC hindcasts. Models such as GFDL_FLORA and FLORB have a positive bias in both periods and the positive bias increases in the second period. For all the initial conditions, the standard deviation is always overestimated by models such as CanCM4i, CanSIPSv2, CCSM3, GFDL_aero4 and GMAO6. GFDL_FLORA has slightly reduced interannual variability than observed variability except for NOV IC hindcasts. CCSM4 also has reduced interannual variability for all ICs considered except for MAY IC.

Thus all the models have decreased interannual variability similar to observations, but ther is more intermodal difference for both the target seasons and lead hindcasts.

b) ENSO skill- actual and potential- .

In the present section, the ability of the models to predict the JJAS and DJF season Nino3.4 index is analysed using correlation for actual and based on RE values for potential skill (equations 1 and 2) and is shown in Table 2. CanCM4i model has a decreased JJAS Nino3.4 index skill for both Feb and May IC hindcasts, while the decrease is stronger (~0.1) for Feb IC. Potential skill is always higher than actual skill, but it has also decreased for Feb IC in recent years. CanSIPSv2 also has a similar reduction of Nino3.4 skill, but the actual skill drop is around 0.2 for Feb IC, while the potential skill drop is around 0.1. The potential skill remains the same in both epochs for May IC and the actual skill decrease is of the order of 0.1 for the 2001-2019 period. CCSM3 has a decrease of 0.28 for JJAS Nino3.4 simulated with Feb IC and 0.20 for May IC with a reduction of 0.15 for Feb IC and 0.08 for May IC potential skills. Feb IC skill loss during the second period is non-significant for models such as CCSM4, GFDL_aero4, FLORA and FLORB. But the actual value is less than 0.6 for GFDL models and is 0.63 for CCSM4. GMAO6 has a decrease of ENSO skill of around 0.15 for both ICs, while potential skill remains the same during both periods. NEMO model, which has a skill of 0.65 for Feb IC during the first period, decreased to 0.29 after 2000 with a decrease of 0.35, while May IC, the skill change is 0.10. The potential skill is high and unchanged during both periods. Thus it is evident that actual skill drops mainly for Feb IC for all models except the GFDL family models, while the maximum decrease is for NEMO and CCSM3. The skill decrease is less for May IC for all models but is relatively higher for GFDL models. Another exciting thing is that potential skill has not much change for May IC and even for Feb IC, the change is very less and is limited to CanSIPSv2, CCSM3, CCSM4 and GFDL_aero4 only.

The same skill comparison for DJF season using Aug (4-month) and Nov (1month) lead ICs are also performed to see whether the same skill drop is applicable for the mature phase of ENSO also. Table 1 shows that compared to JJAS season, the skill drop is negligible for DJF season for both 4 months and 1-month hindcasts. The skill change is always less than 0.05 for 4 months lead itself and also potential skill has no change for both the lead time hindcasts of DJF season ENSO. Thus the skill change of ENSO is mainly concentrated to JJAS season (developing phase of ENSO) and is higher for spring initiation of the hindcasts and so JJAS season is focused rest of the paper. Here we discuss all the changes for all the models for the JJAS target season. Still, only CanCM4i (model with higher skill during period 1 and decreased for period 2), CCSM3 and NEMO (models with the large decrease of skill), CCSM4 (model with less difference between periods) and GFDL_FLORA (having increased skill for Feb IC during period 2) are shown in the following sections.

The analysis of potential skill in these two periods for individual models indicates that definitely, models have room for improvement. Still, the decrease of potential skill for both ICs are marginal or even nill in some cases indicating that the decrease in skill is not directly related to any model deterioration instead model response to the observed climate variability may be the crucial factor. The calculation of Pot. skill itself indicates the role of ensemble spread and ensemble mean in the skill and maybe the combination of these two are not leading to decreased skill, while the actual skill based on ensemble mean only shows a decreased skill.

c) *Role of initial SST anomalies in ENSO skill in both the periods.*

In the present section, the role of initial SST anomalies in the ensemble mean and observations of JJAS Nino3.4 are analysed with the help of correlation analysis. Here Nino3.4 SST indices from both observations and model hindcasts are correlated with the observed initial month SST anomaly. For eg, for Feb IC hindcasts, JJAS nino3.4 index is correlated with February observed SST and for May IC it is May month initial SST. The same analysis for the JJAS Nino3.4 index with February initial SST for observations and Feb IC hindcasts are shown in Figure 1 and the same with May initial SST are shown in figure 2. The observed summer Nino3.4 SST indices have a stronger relationship with off equatorial SSTA in the tropical Pacific, north Indian Ocean (IO) SSTA of February initial month during both the periods (Fig 1 a and b). Additional significant correlation with tropical north Atlantic SST anomalies appears in the second period for February initial conditions. Meanwhile, for May IC, the correlation appears mainly in the tropical east Pacific in both the periods and as of Feb IC, after 2000s North Atlantic SST also plays a role (Fig 2 and b).

The same analysis with model hindcasts shows that CCSM3 and CCSM4 have off equatorial patterns in the Pacific during period1 for February initial SST anomalies, while GFDL_FLORA and NEMO have a strong equatorial pattern at the tropical east Pacific. After 2000, CanCM4i, CCSM4,

GFDL_FLORA have off-equatorial patterns and also have strong anomalies in the north Indian Ocean and north Atlantic (Fig 1c-j). NEMO model has an opposite pattern in both Indian and north Atlantic regions (Fig 1j). Meanwhile, the major contribution from May initial SST is from the equatorial east Pacific for all the models during both periods, while the role of north Atlantic in the second period is captured by CanCM4i, CCSM4 and GFLD_FLORA model only (Fig 2c-j). Models such as CanSIPSv2 and GFDL_FLORB also simulates the role of Atlantic SST, while GMAO6 and GFDL_aero4 fail to do so (not shown).

d) ***Different roles of north and equatorial Atlantic SST anomalies on summer ENSO in both the periods***

The influence of NA_SST of the spring season is confined to the central Pacific as a result of opposite easterly and westerly wind response in the western and eastern Pacific (Ham et al 2013a and the references therein). Meanwhile, the ATL SST anomaly during the boreal summer influences the canonical ENSO and is through modification of Walker circulation (Ham et al 2013a, Rodriguez-Fonseca et al 2009). Figure 2 also indicates the increased influence of Atlantic SST initial state in ENSO evolution and here we analyses whether these SST anomalies induce difference in ENSO evolution in these two periods.

Figure 3 shows the regression of MAM season NA_SST on observed and Feb IC simulated JJAS tropical SST for both periods. The NA_SST regressed anomalies during P1 shows central Pacific ENSO pattern as shown by earlier studies, while during P2, the equatorial pattern has cooling in both east and central Pacific with an extension to off-equatorial east Pacific (Fig 3 a& b). Thus the spatial pattern indicates a clear shift of NA_SST influence from central Pacific to canonical ENSO pattern in the second period. The same is confirmed with the correlation analysis between the indices in table 3 for observations. The NA_SST correlation with Nino3 is increased from 0.06 of pre-2000 value to -0.62 during P2 and that with EMI (index representing El Nino Modoki as defined in Ashok et al 2007) is reduced from -0.56 to -0.36. Negative anomalies of NT_SST is associated with El Nino years such as 1986, 1991, 1994 during period1, which are central Pacific events during that time, while after 2000, the NT_SST has an association with El Nino years such as 2007, 2009, 2010 and 2014, which has canonical type pattern, even with the subtropical extension. The central Pacific ENSO events of 2002, 2004 and 2006 have no significant anomalies in the north Atlantic during the spring season. In our seasonal prediction runs, the NA_SST anomalies are available for the FebIC hindcasts only and the NA_SST analysis is repeated for Feb IC hindcasts of the model. MAM season NA_SSTA induced pattern during period 1 has no proper central Pacific pattern for any of the model hindcasts. But CanCM4i, CCSM4 and FLORA models have cooling in the equatorial central Pacific without tripole pattern. During the second period, cooling is evident in the equatorial east Pacific for all models except NEMO. But the off-equatorial pattern is evident for FLORA model only. Also, the SST pattern in other oceans such as the Indian Ocean is opposite for all the models (Fig 3c-j). In CanSIPSv2 and GMEO6 also has no pattern, while, GFDl_aero4 has warming pattern during period 2 and FLORB has similar pattern as FLORA. Thus the majority of the models fail to capture the NA_SSTA effect on the Pacific Ocean during period2.

The JJAS season SST anomalies obtained by the regression of JJAS ATL SST anomalies for observations and Feb IC and for May IC are shown in Figures 4 and 5. The observed summer season ATL SST anomalies have an almost similar pattern in both the periods with earlier reported canonical ENSO pattern with maximum slightly shifted to central pacific (Fig 4 a&b). The correlation analysis also indicates an almost similar correlation with Nino3 and Nio3.4 in both periods, while EMI has a very low correlation during both periods (Table 3). During period 1, all the model hindcasts from Feb IC has stronger SST pattern in the tropical east Pacific for ATL_SST induced pattern except for CCSM3 and NEMO. The second period has a weak pattern for GFDL_LORB, GMAO6, CanSIPSv2, CCSM3 and GFDL_FLORA hindcast, while others have opposite patterns to that of the observed (Fig 4c-j). At the same time, the May IC hindcasts have cool east Pacific for all the models during period1. But the pattern is weak for CCSM3 and FLORA during period2 and is opposite for NEMO model (Fig 5c-j). Thus, models have better predictability with equatorial Atlantic SST induced pattern as it has a similar pattern as canonical ENSO, while the changes associated with NA_SST are not proper in the majority of the models. The models with a better pattern of NA_SST and ATL induced SST pattern in the Pacific has the better role of initial SST from Atlantic in Figure 2 also.

e) ***Process leading to observed change of NAT_SST in equatorial Pacific***

Another important question here is that why the observed central Pacific ENSO like pattern induced by NA_SST extended to the east Pacific also during the second period? The present section analyses the reason behind the observed change of NA_SST induced SST pattern from central Pacific ENSO to east Pacific after 2000. Figure 6 shows the 850 hPa circulation and 200 hPa velocity potential for MAM and JJAS seasons for the positive minus negative NA_SST composites for both periods. It can be seen that before 2000, positive NA_SST anomalies induces upper-level divergence (lower-level convergence) over the extreme east Pacific and opposite patterns in the central and east Pacific. This is associated with a westerly anomaly in the east Pacific. By summer, this pattern weakens, and convergence moves to the Atlantic but has persistent westerly wind anomalies at east Pacific and easterly anomaly at central Pacific. This is associated with the observed SST pattern in figure 3a earlier and is documented in Ham et al (2013a) Fig 2 also. At the same time after 2000, the NA_SST induced MAM pattern has weaker lower-level convergence and is located at the north Atlantic only with divergence in the equatorial central Pacific. This induces easterly wind anomalies in the east Pacific, opposite to the pre-2000 pattern. The convergence pattern weakens by summer, but the easterly wind anomalies persist in the equatorial region induced cool SST anomalies from east Pacific to central Pacific as observed earlier. The correlation analysis of previous DJF Nino3.4 and spring season NA_SST indices indicates that the correlation is reduced from 0.63 to 0.33 in the second period. This

indicates that the influence of previous winter ENSO on NA_SST, which is the main modulator of spring season NA_SST is also weakened. Thus, we can conclude that the displacement of NA_SST pattern and associated circulation and convection during the boreal spring season during period 2 is responsible for the different effects of North Atlantic SST in equatorial SST in JJAS season. As the role of NAT_SST in CP ENSO reduces after 2000, it seems that the earlier proposed mechanisms involving the ocean role may be responsible for more number of central Pacific ENSO in the recent period (Chung and Li 2013). This needs further analysis also.

f) Spatial SST pattern associated with ENSO

The analysis of Nino3.4 indices for both models and observations indicates that during the first period, there are 5 El Nino (1982, 1987, 1991, 1994 and 1997) and 6 La Nina (1985, 1986, 1988, 1989, 1998, 1999) events are reported during JJAS and it attained its maximum anomaly by DJF. The majority of the models was able to capture these ENSO years and is reflected in the higher skill of the models. Meanwhile during the second period, only the 2015 El Nino is captured by all the model hindcasts, while the El Nino years of 2002, 2004, 2006, 2009, 2014, 2018 have not been obtained by the models, mainly during its growing stage of JJAS season. The observation pattern indicates that the above-mentioned years which the model does not capture are mainly the central Pacific events. Similarly, during period 1 also, models misrepresented the central Pacific events such as 1983, 1994, 1984, 1999, 1998 etc as canonical events or non-ENSO events. Thus, instead of looking at all ENSO events together, here we analyzed the positive minus negative year composite of these years, which are not simulated by the models and is shown in figure 7.

During period 1, the composite has central Pacific warming in observations extending to the north east Pacific with significant cooling in the tropical eastern Pacific. There is strong cooling in the north Atlantic and the eastern Indian Ocean regions. After 2000, the CP El Nino has no significant cooling in the equatorial eastern Pacific and the central Pacific warming extends east. The anomalies are decreased in the tropical Atlantic and are opposite in the east Indian Ocean region. The majority of the models captured the central Pacific El Nino years as canonical ENSO patterns during period1. NEMO model has closer to observed pattern along with CCSM3 model. Earlier we have observed that these two are models with maximum cold bias in the ENSO region and that also can cause westward displacement of ENSO warming as shown by Pillai et al (2017), But after 2000, the equatorial warming is not captured by most of the models and they have maximum warming south of equator mainly for Feb IC and CanCM4i, CCSM4 and FLORA models have stronger central Pacific warming. Also in both periods, these models are not able to capture the signal from the Atlantic and the Indian Ocean properly.

Thus, during period1, the models captured the central Pacific ENSO as similar to canonical ENSO, but the events were very less in number. But after 2000, when most of the events are CP ENSO except 2007, 2010, 2015 etc, the models failed to capture the elongated pattern of warming, mainly for Feb IC. This also can induce reduced skill and interannual variability of ENSO in the models.

4. Summary And Conclusion

The present study analyses the skill difference of El Nino Southern Oscillation (ENSO) in the recent period using NMME hindcast for 1-month and 4-month lead hindcasts for boreal summer (JJAS) and boreal winter (DJF). We have used Nino3.4 region SST anomalies to represent the ENSO in both model and observations. Initial analysis indicates that all the models have reduced interannual variability during period2 in both the seasons and is in accordance with the observations. Thus, the models simulate the observed decrease in interannual variability of ENSO after 2000. The cool bias of most of the models reduced slightly during period 2, while the GFDL-FLORA model has a positive bias in both periods. The skill (anomaly correlation between the ensemble mean ENSO index and observed value) analysis indicates that there is an increase of skill with the decrease of forecast lead time in both the periods and seasons. Meanwhile, the majority of the models also have decreased skill for mainly long lead hindcast during period2, while some models have increased skill also. The potential skill also decreases for some models after 2000, but it is limited to Feb IC hindcast for the JJAS season. But some models such as CCSM4 has a very small reduction in skill (~0.04), while the models such as CCSM3, NEMO etc has a reduction of around 50% for Feb IC and the GFDL models have increased skill for Feb IC and that of May IC decreased slightly. Similarly, skill decrease of DJF ENSO for both the lead hindcasts is not significant for the models.

Further analysis of the influence of February SST anomaly on JJAS SST simulation of Nino3.4 region shows off equatorial SST pattern in the Pacific and north IO basin-wide anomalies during both the periods while there is additional SST anomalies in the north and the equatorial Atlantic Ocean during period2. Similarly for May IC also there was a strong equatorial SST pattern in the east Pacific during both periods and additional stronger SST anomalies in the equatorial Atlantic. The majority of the models captures the off-equatorial pattern for Feb IC in the pacific, but the north Atlantic SST pattern is weaker during period2, except for CanCM4i, CCSM4 and GFDL_FLORA models. May IC has an equatorial ENSO like pattern for models also, but the role of north Atlantic SST anomalies is limited. Thus, many models have a problem in simulating the role of spring season Atlantic initial SST for simulation of the JJAS ENSO SST.

Earlier studies already indicated that north Atlantic SST anomalies in the spring season influence the central Pacific SST anomalies during the summer season and ENSO evolution. Meanwhile, our study indicates that the spring NA_SST induces central Pacific pattern during period 1 and the SST anomalies tend to extend east Pacific during period2, indicating a higher correlation between Nino3 and NA_SST during that period.

This observed change in the tropical Pacific SST pattern is associated with the weakening and northward shift of NA_SST induced convergence during the spring season during the P2. Almost all the models fail to capture the relationship in both the periods, while CCSM4 and FLORA model has some cooling in the east and central Pacific during period1 and the extension of central and east Pacific cooling to off equatorial noth Pacific is only for FLORA during period 2 for Feb IC hindcasts. At the same time, cooling in the eastern Pacific is evident for most of the models during period 1 except NEMO and FLORA for Feb IC and for all models for May IC. But after 2000, it is weak for almost all the models. Also, models have opposite anomalies in the IO region for both the Atlantic SST anomalies. Thus, the interaction of Atlantic SST anomalies to the east Pacific is not proper in the models and is worse and opposite for NEMO and is somewhat close to observations for FLORA followed by CCSM4, both of which has a higher skill for ENSO during period2. It is also to be noted that these two are the models with better representation of the role of February initial SST in ENSO in figure 2.

The models also fail to capture the majority of El Nino events in the second period, which are mainly central Pacific events and the warming associated with the ENSO are shifted far westward and is south of the equator mainly. During first period also Feb IC hindcasts are not able to simulate the central Pacific ENSO events, but are less in number only and so the skill deterioration due to the inability to capture central Pacific ENSO are less. Here we may can assume that during the second period, there is only one strong ENSO event such as 2015, while during P1 there are events such as 1987-1988, 1997 and more east Pacific ENSO events with more predictability. But during P2 there are more central Pacific events, which may not provide much long-range predictability. This itself can lead to the decline of skill. But here the models whose skill have more reduction during period2 failed to capture the role of initial SST anomalies in the tropical Atlantic and their interaction with east Pacific SST anomalies. Thus, the inability of the model to capture the changes tropical Atlantic Ocean SST pattern during spring and summer is a major issue for the models for their reduced skill of ENSO.

Declarations

Acknowledgements: Authors are thankful to Prof. Ravi S. Nanjundiah, Director, Indian Institute of Tropical Meteorology (IITM) and Dr Suryachandra A Rao, Program manager, Monsoon Mission, IITM for encouraging to carry out this research work. The IITM is fully funded by the Ministry of Earth Sciences, Government of India. All the figures are prepared using GrADS software freely available from http://cola.gmu.edu/grads/

Funding Information: Authors have no funding information

Data availability: All the observed data sets used are available online downloadable from ECMWF (atmospheric variables) https://www.ecmwf.int/en/forecasts/datasets/reanalysis-datasets/era5., HadISST from https://www.metoffice.gov.uk/hadobs/hadisst/data/download.html and model out puts from http://iridl.ldeo.columbia.edu/SOURCES/.Models/.NMME/.

Competing Interests

The authors declare no competing interests.

Author's contribution

P.A Pillai- Conceptualisation, Formal analysis, supervision, methodology and validation., writing-original, reviewing and editing. A. R Dhakate- Validation, Software, writing -corrections and editing.

Code availability:

Not applicable

Ethics Declaration

Ethics Approval:

Not applicable.

Consent to participate:

Not applicable

Consent to publish

Not applicable.

Conflict of Interest

The authors have no conflicts of interest to declare.

References

1. Ashok K, Behera S, Rao AS, Weng H, Yamagata T (2007) El Niño Modoki and its teleconnection. J Geophys Res 112:C11007. doi: 10.1029/2006JC003798
2. Balmaseda M, Anderson D, Vidard A (2007) Impact of Argo on analyses of the global ocean. *Geophys Res Lett***34:**L16605. doi:10.1029/2007GL030452.
3. Balmaseda M, Mogensen K, Weaver A (2013) Evaluation of the ECMWF ocean reanalysis ORAS4. *Quart J Roy Meteor Soc***139:**1132–1161. doi:10.1002/qj.2063.
4. Barnston AG, Tippett MK, L'Heureux ML et al (2012) Skill of real-time seasonal ENSO model predictions during 2002–11: Is our capability increasing?. *Bull Amer Meteor Soc***93:**631–651. doi:10.1175/BAMS-D-11-00111.1.
5. Choi, J., An SI, Yeh SW (2011), Decadal amplitude modulation of two types of ENSO and its relationship with the mean state. Clim. Dyn 38, 1-14.
6. Chung P-H, Li T (2013) Interdecadal relationship between the mean state and El Niño types. *J Climate***26:**361–379. doi:10.1175/JCLI-D-12-00106.1.
7. Feng, M M, McPhaden, J, Lee T (2010) Decadal variability of the Pacific ubtropical cells and their influence on the southeast Indian Ocean, *Geophys. Res. Lett.*, **37**, L09606, doi:10.1029/2010GL042796.
8. Ham YG, Kug JS, Park JY(2013a). Two district roles of Atlantic SSTs in ENSO variability: North Tropical Atlantic SST and Atlantic Nino. Gophy. Res. Lett 40, 4012-4017.
9. Ham YG, Kug JS, Park JY, Jin FF (2013b) Sea surface temperature in the north tropical Atlantic as a trigger for El Niño/Southern Oscillation events. Nature Geosci 6:112–116. https://doi.org/10.1038/ngeo1686.
10. Hendon HH, Lim E, Wang G, Alves O, Hudson D (2009) Prospects for predicting two favours of El Niño. Geophys Res Lett 36:L19713
11. Hersbach, H, co-authors. (2020). The ERA5 global reanalysis. *Quart. J. Royal. Met.Soci.* 146, 1999-2049.
12. Hu Z-Z, Kumar A, Ren H-L, Wang H, Heureux ML, Jin FF (2013) Weakened interannual variability in the tropical Pacific Ocean after 2000. *J Climate***26:**2601–2613, https://doi.org/10.1175/JCLI-D-12-00265.1.
13. Izumo T, co-authros (2016) A simple estimation of equatorial Pacific response from windstress to untangle Indian Ocean dipole and basin influences on El Niño. Clim Dyn 46(7-8): 2247–2268. https://doi.org/10.1007/s00382-015-2700-4.
14. Jin F-F (1997) An equatorial ocean recharge paradigm for ENSO. Part I: Conceptual model. J Atmos Sci 54: 811–829. https://doi.org/10.1175/1520-0469(1997)054<0811:AEORPF>2.0.CO;2.
15. Kirtman B, Schopf PS (1998) Decadal variability in ENSO predictability and prediction. *J Climate***11:** 2804–2822. https://doi.org/10.1175/1520-0442(1998)011<2804:DVIEPA>2.0.CO;2.
16. Kleeman R (2002) Measuring dynamical prediction utility using relative entropy. J Atmos Sci 59:2057–2072
17. Kug J-S, Kang I-S (2006) Interactive feedback between the Indian Ocean and ENSO. J Clim 19: 1784–1801.
18. Kumar A, Chen M, Xue Y, Behringer D (2015) An analysis of the temporal evaluation of ENSO prediction skill in the context of equatorial Pacific Ocean observing system. *Mon Wea Rev***143:** 3204–3213, https://doi.org/10.1175/MWR-D-15-0035.1.
19. Luo J-J, Zhang R, Behera SK, Mastumoto Y, Jin FF, Lukas R, Yamagata T (2010) Interaction between El Niño and extreme Indian Ocean dipole. J Clim 23: 726–742.
20. Luo J-J, Sasaki W , Masumoto Y (2012) Indian Ocean warming modulates Pacific climate change. *Proc Natl Acad Sci USA***109**, 18:701–18 706. https://doi.org/10.1073/pnas.1210239109.
21. McPhaden MJ, Zebiak SE, Glantz MH (2006) ENSO as an integrating concept in Earth science. Science 314: 1740–1745. https://doi.org/10.1126/science.1132588.
22. McPhaden MJ (2012) A 21st century shift in the relationship between ENSO SST and warm water volume anomalies. Geophys Res Lett 39: L09706. doi:10.1029/2012GL051826.
23. McPhaden MJ, Lee T, McClurg D (2011) El Niño and its relationship to changing background conditions in the tropical Pacific Ocean. Geophys Res Lett 38: L15709. https://doi.org/10.1029/2011GL048275.
24. Pillai PA., Rao SA , Das R.S., Salunke K, Dhakate A (2018). Potential predictability and actual skill of Boreal Summer Tropical SST and Indian summer monsoon rainfall in CFSv2-T382: Role of initial SST and teleconnections. Clim. Dyn.51. 493-510

25. Pillai, P. A., Rao, S. A., George, G., Rao, D. N, Mahapatra, S., Rajeevan, M., Dhakate, A, Salunke, K. (2017). How distinct are flavors of El Nino in retrospective forecasts of climate forecast system version2(CFSv2)?. *Clim. Dyn*., 48, 3829-3854.
26. Rayner NA, co-authros (2003) Global analyses of sea surface temperature, sea ice, and night marine air temperature since the late nineteenth century. J Geophys Res 108:4407. doi:10.1029/2002JD002670, D14.
27. Rodriguez-Fonseca B, Polo I, Gracie-Serrano J, Losada T, Mohino E, Mechoso CR, Kucharski Fl (2009) Are Atlantic Niños enhancing Pacific ENSO events in recent decades?. Geophys Res Lett 36: L20705.
28. Saha S, co-authors (2014) The NCEP Climate Forecast System version 2. *J Climate* **27:**2185–2208. https://doi.org/10.1175/JCLI-D-12-00823.1.
29. Wang C, Kucharski F, Barimalala R, Bracco A (2009) Teleconnections of the tropical Atlantic to the tropical Indian and Pacific Oceans: a review of recent findings. Meteorol Z 18:445–454
30. Wen C, Kumar A, Xue X, McPhaden MJ (2014) Changes in tropical Pacific thermocline depth and their relationship to ENSO after 1999. *J Climate* **27**:7230–7249. https://doi.org/10.1175/JCLI-D-13-00518.1.
31. Xiang B, Wang B, Li T (2013) A new paradigm for the predominance of standing central Pacific warming after the late 1990s. *Climate Dyn* **41:**327–340. https://doi.org/10.1007/s00382-012-1427-8.
32. Zhao M, Hendon H, Alves O, Yin YH (2014) Impact of improved assimilation of temperature and salinity for coupled model seasonal forecasts. *Climate Dyn* **42:**2565–2583. doi:10.1007/s00382-014-2081-0.
33. Zhao M, Hendon H, Alves O, Yin YH, Anderson, D (2013) Impact of salinity constraints on the simulated mean state and variability in a coupled seasonal forecast model. *Mon Wea Rev* **141:** 388–402. doi:10.1175/MWR-D-11-00341.1.

Tables

Table 1: Bias (deg.C) and standard deviation of individual models for both the JJAS and SON season from two initial conditions for both the periods.

Models	JJAS season								DJF season							
	Feb IC				May IC				Aug IC				Nov IC			
	Period1		Period2		Period1		Period2		Period1		Period2		Period 1		Period 2	
	Bias	SD	Bias	SD	Bias	SD	Bias	SD	Bias	SD	Bias	SD	Bias	SD	Bias	SD
CanCM4i	-0.90	1.08	-0.74	0.85	-0.92	1.25	-0.83	0.99	-0.76	1.55	-0.39	1.30	-1.0	1.62	-0.75	1.49
CanSIPSv2	-1.76	0.86	-1.67	0.60	-1.38	0.96	-1.37	0.65	-1.23	1.35	-0.79	1.01	-1.3	1.38	-1.17	1.22
CCSM3	-2.7	0.80	-1.7	0.66	-1.96	1.17	-1.92	0.71	-1.32	1.29	0.01	1.11	-1.3	1.4	-0.42	1.23
CCSM4	-0.3	0.73	0.08	0.67	-0.67	0.88	-0.11	0.76	-0.11	1.14	1	1.04	-0.34	1.05	0.41	0.94
GFDL_aero4	-2.1	1.06	-1.2	0.7	-1.6	1.07	-1.25	0.8	-0.88	1.38	-0.07	0.86	-0.62	1.62	-0.05	1.23
GFDL_FLORA	0.5	0.65	1.17	0.43	0.16	0.63	0.46	0.43	0.78	1.09	1.54	0.96	0.39	1.32	0.88	1.17
GFDL_FLORB	0.37	0.81	1.05	0.65	0.05	0.92	0.49	0.76	0.82	1.05	1.57	0.93	0.43	1.27	0.89	1.14
GMAO6	-1.0	0.82	-0.7	0.65	-0.96	1.09	-0.67	0.94	-2.0	1.44	-1.01	1.12	-0.99	1.68	-0.55	1.43
NEMO	-2.6	0.84	-2.6	0.59	-1.37	0.93	-1.39	0.65	-1.67	1.15	-1.12	0.96	-1.28	1.38	-1	

Table 2: Actual skill (anomaly correlation between observed and ensemble mean Nino3.4 index) of ENSO for JJAS and DJF seasons from both lead forecasts for period 1 and period 2 for individual models. The value in bracket corresponds to the potential skill for same. The models with bold phase are the models used for further analysis.

Models	JJAS season				DJF season			
	Feb IC		May IC		Aug IC		Nov IC	
	Period1	Period2	Period1	Period2	Period1	Period2	Period 1	Period 2
CanCM4i	0.72(0.90)	0.63(0.86)	0.86(0.94)	0.82(0.90)	0.92(0.96)	0.89(0.95)	0.95(0.97)	0.95(0.97)
CanSIPSv2	0.71(0.89)	0.58(0.80)	0.85(0.95)	0.78(0.95)	0.94(0.98)	0.90(0.98)	0.90(0.98)	0.95(0.98)
CCSM3	0.77(0.85)	0.50(0.78)	0.83(0.95)	0.63(0.89)	0.90(0.97)	0.84(0.95)	0.94(0.98)	0.91(0.98)
CCSM4	0.64(0.85)	0.61(0.81)	0.85(0.92)	0.80(0.91)	0.79(0.95)	0.83(0.95)	0.91(0.96)	0.92(0.96)
GFDL_aero4	0.53(0.89)	0.58(0.86)	0.76(0.94)	0.64(0.92)	0.80(0.96)	0.88(0.96)	0.82(0.97)	0.90(0.97)
GFDL_FLORA	0.47(0.86)	0.60(0.92)	0.81(0.94)	0.76(0.93)	0.89(0.96)	0.87(0.96)	0.94(0.97)	0.96(0.98)
GFDL_FLORB	0.47(0.90)	0.56(0.92)	0.81(0.92)	0.72(0.95)	0.90(0.93)	0.87(0.95)	0.94(0.97)	0.95(0.97)
GMAO6	0.75(0.90)	0.60(0.89)	0.85(0.93)	0.72(0.92)	0.89(0.95)	0.89(0.95)	0.95(0.98)	0.95(0.98)
NEMO	0.65(0.93)	0.30(0.90)	0.85(0.94)	0.76(0.95)	0.94(0.96)	0.91(0.95)	0.94(0.97)	0.95(0.97)

Table 3: correlation of boreal spring north Atlantic SST (NAT_SST) and summer season Atlantic Nino SST (ATL_SST) with JJAS Nino3 and EMI for period 1 and period 2. The indices are as defined in the text.

Atlantic SST index	Nino3		EMI	
	Period1	Period2	Period1	Period2
NAT_SST (MAM)	0.06	-0.66	-0.56	-0.35
ATL SST (JJAS)	-0.36	-0.40	-0.25	-0.28

Figures

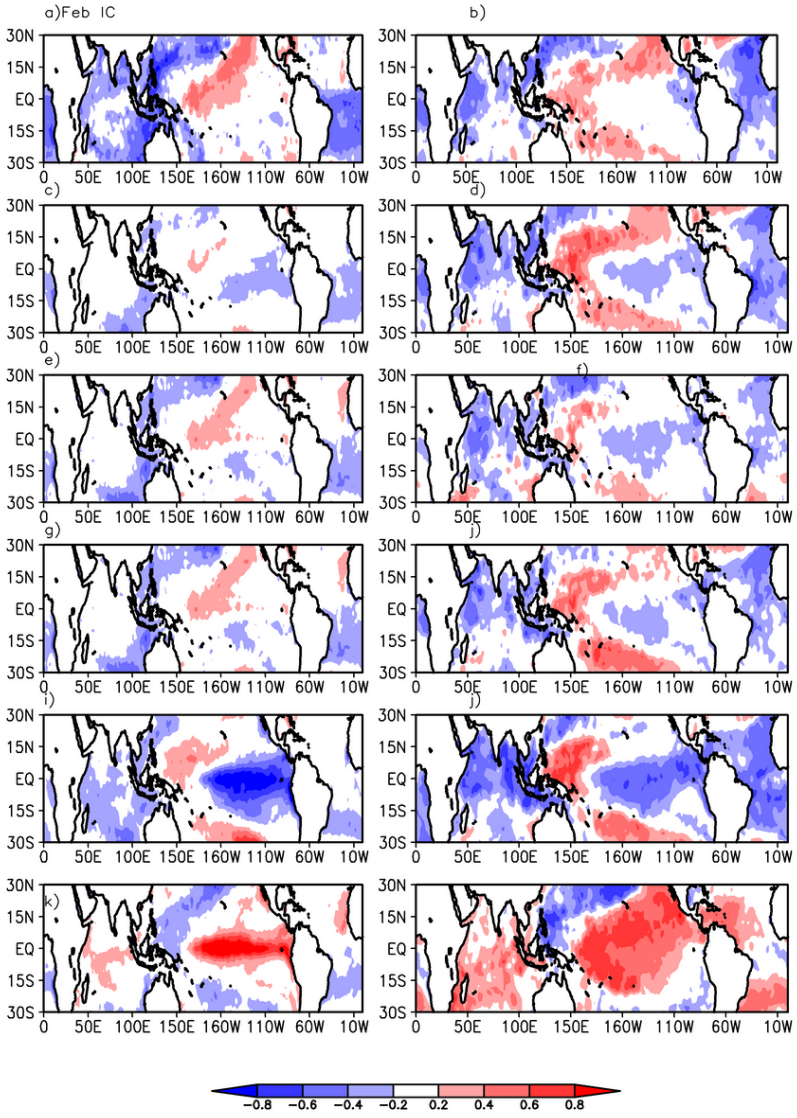

Figure 1

Correlation of JJAS Nino3.4 index with observed February SST for period 1(left panels) and period 2(right panels) for (a) and (b) observations and Feb IC hindcasts of (c)-(d) CanCM4i, (e) and (f) CCSM3, (g) and (h) CCSM4, (i) and(j) GFDL_FLORA and (k)-(l) for NMEO models

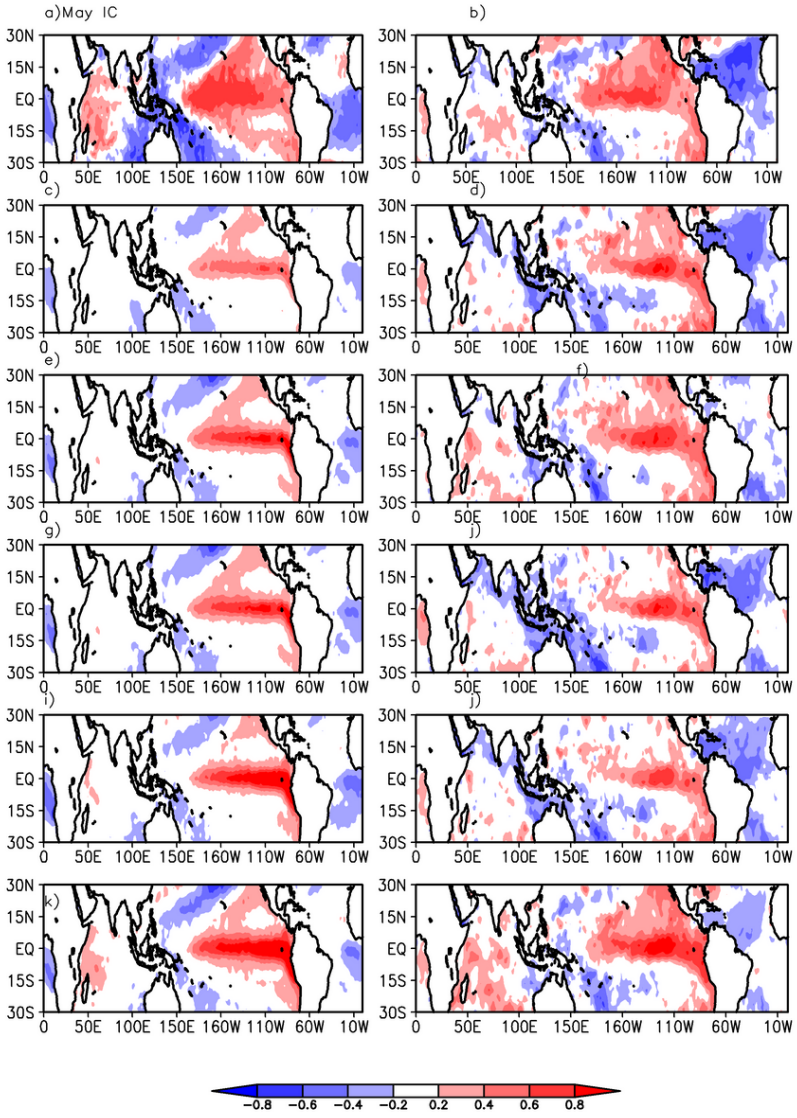

Figure 2

Correlation of JJAS Nino3.4 index with observed May SST for period 1(left panels) and period 2(right panels) for (a) and (b) observations and May IC hindcasts of (c)-(d) CanCM4i, (e) and (f) CCSM3, (g) and (h) CCSM4, (i) and(j) GFDL_FLORA and (k)-(l) for NMEO models

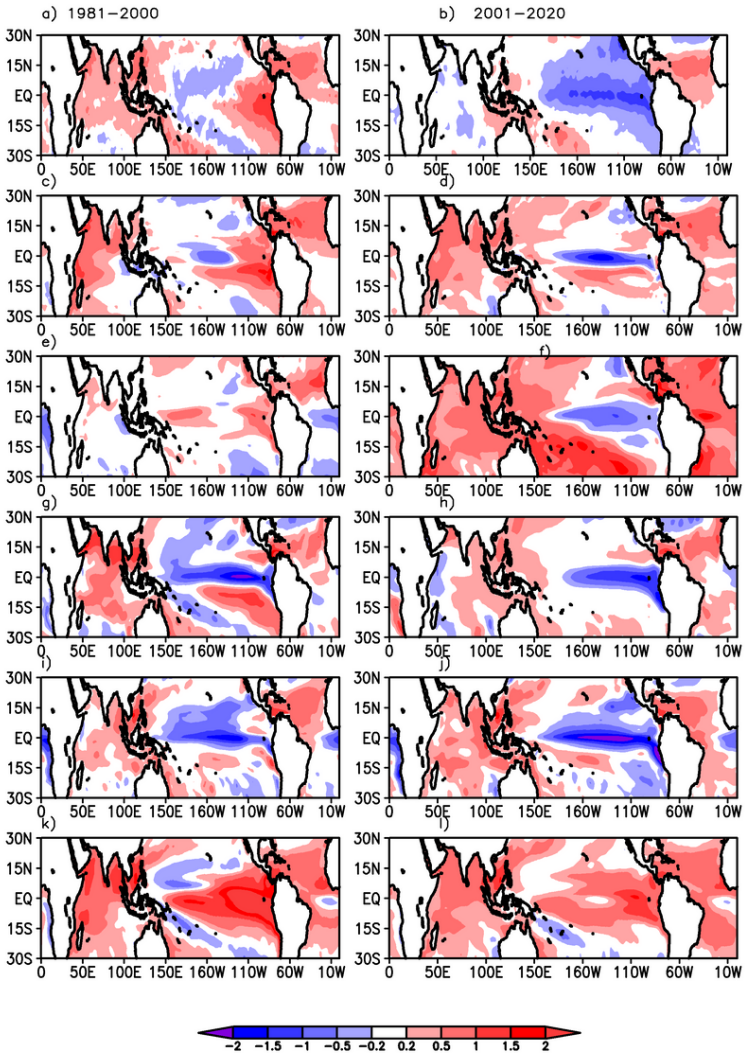

Figure 3

JJAS season SST anomalies (Deg.C) obtained by the regression of North Atlantic (90W-20E, 0-15N) SST anomaly index for period 1(left panels) and period 2(right panels) for (a) and (b) observations and Feb IC hindcasts of (c)-(d) CanCM4i, (e) and (f) CCSM3, (g) and (h) CCSM4, (i) and(j) GFDL_FLORA and (k)-(l) for NMEO models

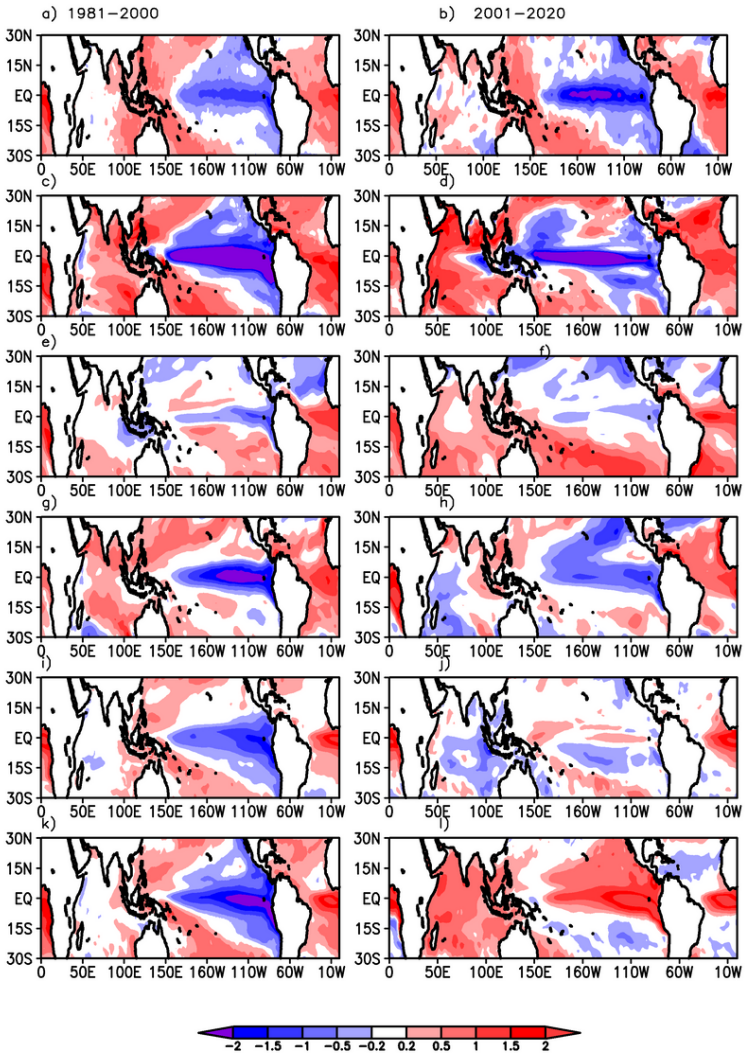

Figure 4

JJAS season SST anomalies (Deg.C) obtained by the regression of tropical Atlantic (90W-20E, 0-15N) SST anomaly index for period 1(left panels) and period 2(right panels) for (a) and (b) observations and Feb IC hindcasts of (c)-(d) CanCM4i, (e) and (f) CCSM3, (g) and (h) CCSM4, (i) and(j) GFDL_FLORA and (k)-(l) for NMEO models

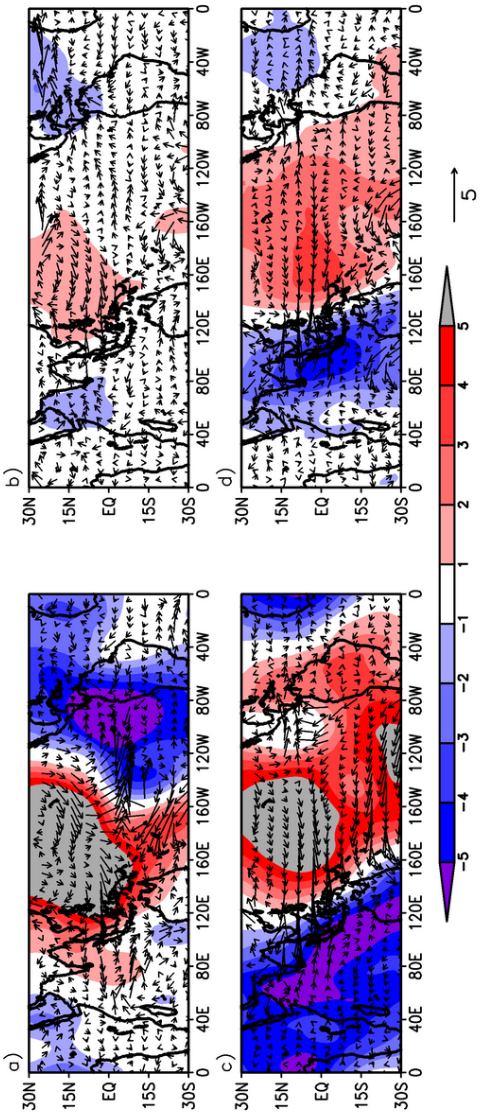

Figure 5

JJAS season SST anomalies (Deg.C) obtained by the regression of tropical Atlantic (90W-20E, 0-15N) SST anomaly index for period 1(left panels) and period 2(right panels) for (a) and (b) observations and May IC hindcasts of (c)-(d) CanCM4i, (e) and (f) CCSM3, (g) and (h) CCSM4, (i) and(j) GFDL_FLORA and (k)-(l) for NMEO models

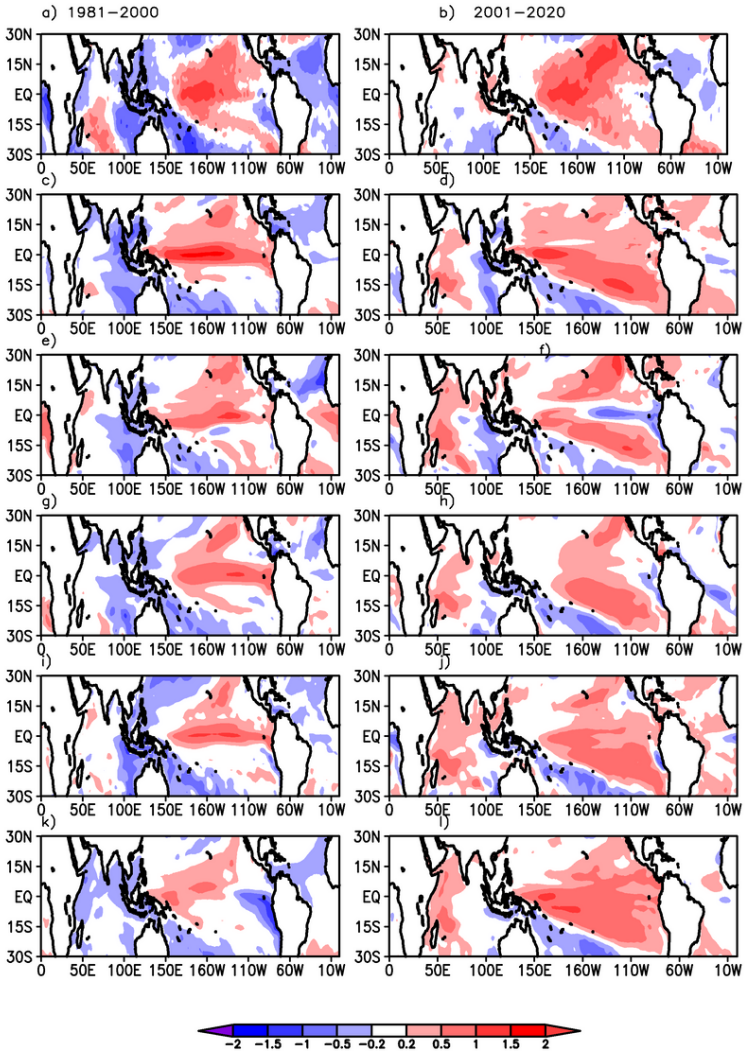

Figure 6

Composite anomalies of 850 hPa wind (vector, m/s) and 200 hpa velocity potential (shaded,–) for strong minus weak years of North Atlantic SST anomaly from observations for period 1(left panel) and period 2(right panel) of (a)-(b) boreal soring (MAM) season and (c)-(d) for boreal summer (JJAS) season

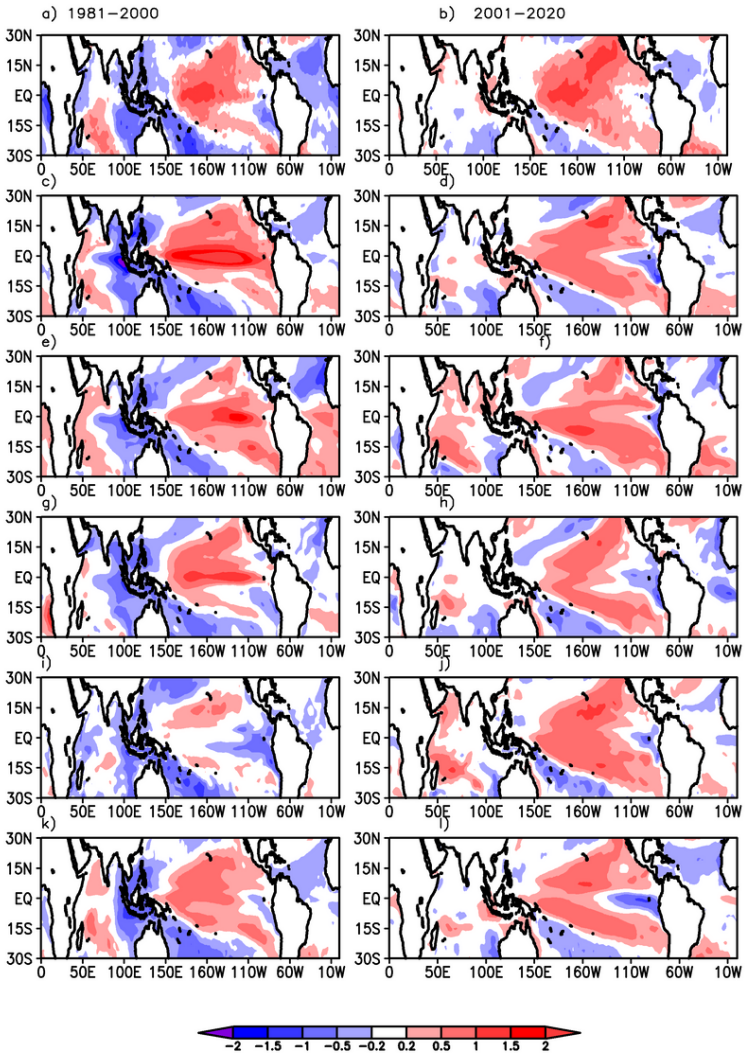

Figure 7

JJAS SST anomalies(Deg.C) associated with strong minus weak composite of central Pacific ENSO events for period 1(left panels) and period 2(right panels) for (a) and (b) observations and Feb IC hindcasts of (c)-(d) CanCM4i, (e) and (f) CCSM3, (g) and (h) CCSM4, (i) and(j) GFDL_FLORA and (k)-(l) for NMEO models

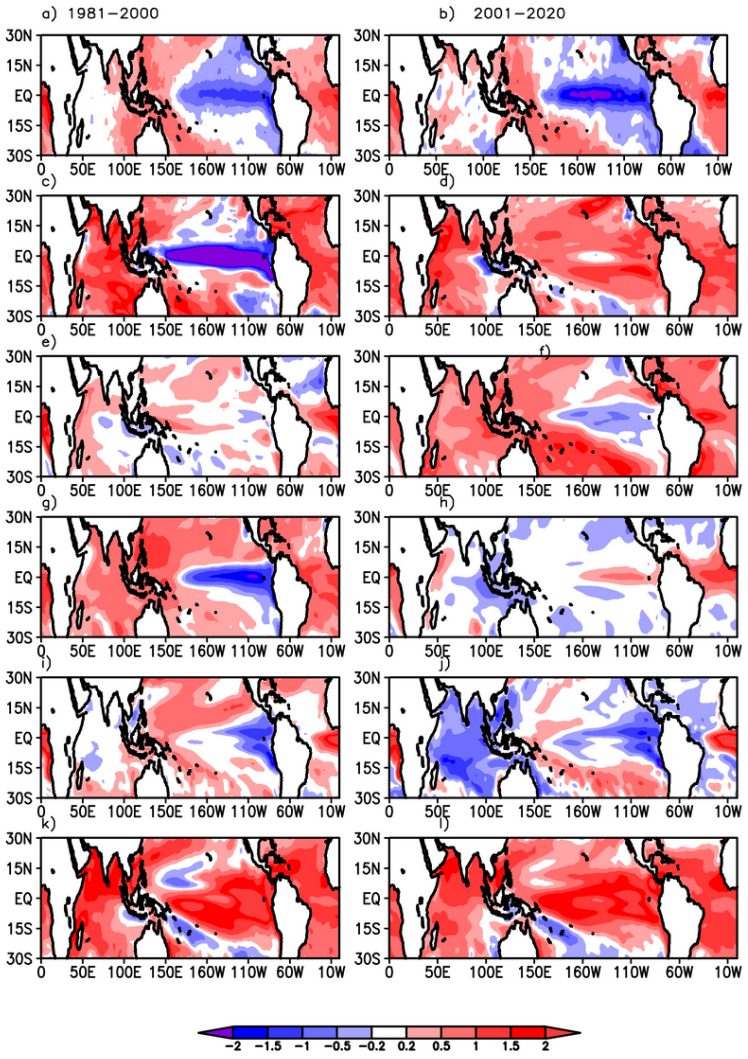

Figure 8

JJAS SST anomalies(Deg.C) associated with strong minus weak composite of central Pacific ENSO events for period 1(left panels) and period 2(right panels) for (a) and (b) observations and May IC hindcasts of (c)-(d) CanCM4i, (e) and (f) CCSM3, (g) and (h) CCSM4, (i) and(j) GFDL_FLORA and (k)-(l) for NMEO models